



Estimation of Land Surface Temperature Using LANDSAT 8 Satellite Data of Panchkula District, Haryana

Ravi Kumar^{1*} and Anup Kumar¹

¹Front Office-HARSAC, Sector-2, Panchkula, India.

Authors' contributions

This work was carried out in collaboration between both authors. Author RK designed the study, performed the statistical analysis, image classification, wrote the protocol, and wrote the first draft of the manuscript. Author AK managed the analyses of the study and managed the literature searches. Both authors read and approved the final manuscript.

Article Information

DOI: 10.9734/JGEESI/2020/v24i1030263

Editor(s):

(1) Dr. Wen-Cheng Liu, National United University, Taiwan.

Reviewers:

(1) Miguel Galván-Ruiz, Autonomous University of Querétaro, Mexico.

(2) Darren How Jin Aik, Universiti Putra Malaysia, Malaysia.

(3) Sergio Meseguer Costa, Jaume I University, Spain.

Complete Peer review History: <http://www.sdiarticle4.com/review-history/66425>

Case Study

Received 20 October 2020
Accepted 27 December 2020
Published 31 December 2020

ABSTRACT

Land surface temperature (LST) represents hotness of the surface of the Earth at a particular location. Land surface temperature is useful for meteorological, climatological changes, heat island, agriculture, hydrological processes at local, regional and global scale. Presently many satellite sensor data are available for calculation of land surface temperature like Landsat 8 and MODIS. In the present study land surface temperature in Panchkula district of Haryana have been calculated using Landsat 8 satellite data of 5th May 2019 and 28th October 2019. Already available equations were used for computation of LST in the study area. LST in the study area varies from 18°C to 56°C. High LST is observed in cultivation land, urban area while low LST is observed in hilly forest area in the study area. In the study validation of LST could not be done because of not available of temperature data of studied dates, however, the result gives idea of land surface temperature on a particular day and location.

*Corresponding author: E-mail: ravigisrs@gmail.com;

Keywords: Land surface temperature; land surface emissivity; Normalized difference vegetation index; Landsat 8; land use; land cover; Panchkula; Haryana.

1. INTRODUCTION

Land surface temperature (LST) is the skin temperature of the surface of the earth and provides important information about the surface physical, bio-physical, climatic, environmental and anthropogenic changes. LST reflects the land surface water-heat exchange process which is considerably significant to the study of environmental change [1]. It is one of the key parameter in understanding the physics of land surface processes from local to global scale. LST changes with a change in climatic condition and other human activities where the exact prediction becomes challenging [2]. Land Surface temperature has identified as a significant variable of microclimate and radiation transfer within the atmosphere [3]. Worldwide urbanization has significantly reshaped the landscape, which has important climatic implications across all scales due to the

simultaneous transformation of natural land cover and anthropogenic surfaces [4]. Land Surface Temperature is an important phenomenon in global climate change. LST will increase as the greenhouse gases in the atmosphere increases [5]. Land surface temperature is sensitive to vegetation and soil moisture, hence, it can be used to detect land use/land cover changes.

1.1 Study Area

In the present study Panchkula District of Haryana state have been selected for variability in topography which have been studied to get relationship between land surface temperature and elevation. Panchkula district lies between the geo-coordinates 30°26'N to 30°55' N latitudes and 76°46'E to 77°10'E longitudes and covers 898 km² area (Fig. 1).

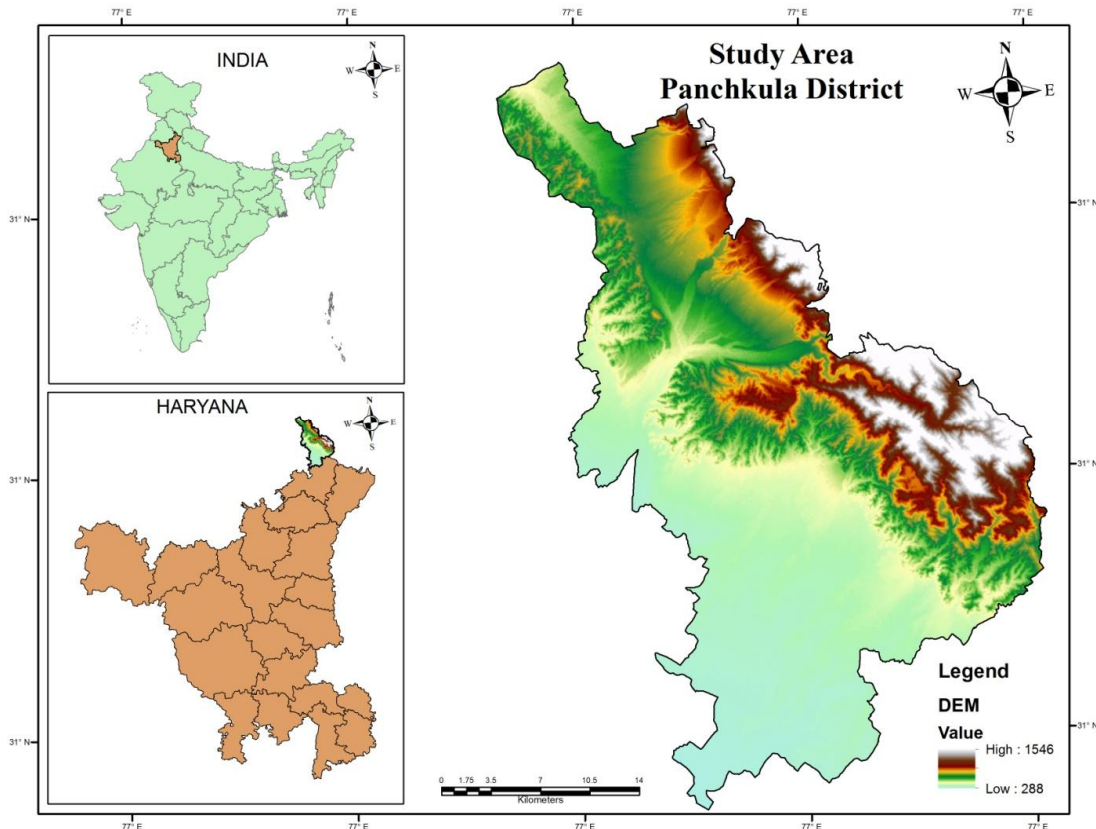


Fig. 1. Location map of the study area.

1.2 Objectives

The main objective of the study was to estimate land surface temperature using Landsat 8 satellite data in the study. The other subsidiary objectives were following to achieve the main Objective:

1. To convert TIRS band data to Top of Atmosphere (TOA) spectral radiance.
2. To calculate Atmosphere Brightness Temperature
3. To calculate Normalized Difference Vegetation Index (NDVI).
4. To generate contour from SRTM DEM.
5. To explore the relationship between LST, different land use types and Elevation Ranges.
6. To calculate the area for different temperature ranges.

2. MATERIALS AND METHODS

2.1 Data Used

Landsat-8 OLI (Operational Land Imager) satellite data of Panchkula district of two dates 5th May, 2019 and 28th October, 2019 (level-I product, path/row 147/39) was downloaded from Earth Explorer (www.earthexplorer.usgs.gov) (Table 1). ArcGIS 10.1 was used for image processing, image correction, clipping of area of interest, preparation of vegetation index and estimation of LST, etc. Landsat 8 metadata of the bands were used for calculation of LST. Images were resampled using nearest neighbor method. All the data were re-projected to Universal Transverse Mercator (UTM) coordinate system, datum WGS84, zone 43. Thermal infrared sensor (TIRS) band 10 was used to estimate brightness temperature and band 4 and band 5 were used to generate NDVI.

3. METHODOLOGY

In this study, TIRS band 10 was used to estimate brightness temperature and band 4 and band 5 were used to calculate normalized difference vegetation index (NDVI). Stepwise process for calculation of LST is given below and also shown in Fig. 1. Shuttle Radar Topography Mission (SRTM) digital elevation model (DEM) data of 30m resolution was downloaded from USGS Earth Explorer website and used for elevation generation in the study area. In this study, LST has been calculated using methods available on USGS webpage

(http://landsat.usgs.gov/Landsat8_Using_Product.php).

3.1 Step 1. Calculation of Top of Atmosphere (TOA) Spectral Radiance [USGS Formula](6)

The satellite data products were geometrically corrected data set. The metadata of the satellite image is given in Table 2. In the first step of the work converted the DN (Digital Number) values of band 10 to at-sensor spectral radiance using the following equation:

Top of Atmosphere (TOA) Radiance:

$$\text{TOA (L)} = M_L * Q_{\text{cal}} + A_L$$

Where

M_L = Band specific multiplicative rescaling factor from the metadata (Radiance_Mult_Band_x, where x is the band number).

Q_{cal} = corresponds to band 10.

A_L = Band specific additive rescaling factor from the metadata (Radiance_Add_Band_x, where x is the band number).

$$\text{TOA} = 0.0003342 * \text{“Band 10”} + 0.1$$

The above equation was solved using the Raster Calculator tool in **Arc Map 10.1**.

3.2 Step 2. TOA to Brightness Temperature (BT) Conversion

The temperature converted from the obtained thermal radiance from the ground surface at the satellite level is called the brightness temperature. After converting DN values to sensor spectral radiance, the TIRS band data were converted to brightness temperature (BT). TIRS band data were converted from spectral radiance to brightness temperature using the thermal constants provided in the metadata file (Table 2). and following equation:

$$\text{BT} = (K2 / (\ln (K1 / L) + 1)) - 273.15$$

Where

K_1 = Band specific thermal conversion constant from the metadata

($K_1_Constant_Band_x$, where x is the thermal band number).

K_2 = Band specific thermal conversion constant from the metadata

($K_2_Constant_Band_x$, where x is the thermal band number).

L = TOA

To obtain the result in degree Celsius, radiant temperature is adjusted by adding the absolute zero temperature (approx.-273.15°C).

$$BT = (1321.0789 / \ln ((774.8853 / "TOA" + 1)) - 273.15$$

3.3 Step 3. Normalised Difference Vegetation Index (NDVI) Calculation

Normalised Difference Vegetation Index (NDVI) was calculated using Near infrared (Band 5) and Red (Band 4) bands. Calculation of NDVI is required for calculation of proportion of vegetation (Pv), further, proportion of vegetation (Pv) is required for calculation of emissivity (ε) and emissivity (ε) is required for calculation of LST. NDVI was calculated using following equation:

$$NDVI = (NIR - RED) / (NIR + RED)$$

$$NDVI = (Band 5 - Band 4) / (Band 5 + Band 4)$$

3.4 Step 4. Proportion of vegetation (Pv) Calculation

Proportional vegetation (Pv) was calculated from

NDVI values obtained in step 3. This proportional vegetation gives the estimation of area under each land use/land cover type.

$$Pv = \text{Square} ((NDVI - NDVI \text{ min}) / (NDVI \text{ max} - NDVI \text{ min}))$$

where

Pv = Proportion of vegetation

NDVI = DN values from NDVI image

NDVI min = Minimum DN values from NDVI image

NDVI max = Maximum DN values from NDVI image

$$Pv = \text{Square} ((NDVI - 0.216901) / (0.632267 - 0.216901))$$

3.5 Step 5. Land Surface Emissivity (ε) Calculation

Land surface emissivity (LSE) is the average emissivity of an element of the surface of the Earth calculated from NDVI. Calculation of land surface emissivity is required to estimate LST.

$$\epsilon = 0.004 * PV + 0.986$$

Table 1. Landsat 8 OLI

Bands	Wavelength (µm)	Resolution (m)
Operational Land Imager (OLI)-Built by Ball Aerospace & Technologies Corporation (Nine spectral bands, including a panchromatic band)		
Band 1-Ultra Blue (Coastal Aerosol)	0.43 - 0.45 µm	30 m
Band 2-Blue	0.45 - 0.51 µm	30 m
Band 3-Green	0.53 - 0.59 µm	30 m
Band 4-Red	0.64 - 0.67 µm	30 m
Band 5-Near Infrared (NIR)	0.85 - 0.88 µm	30 m
Band 6-Shortwave Infrared (SWIR) 1	1.57 - 1.65 µm	30 m
Band 7-Shortwave Infrared (SWIR) 2	2.11 - 2.29 µm	30 m
Band 8-Panchromatic	0.50 - 0.68 µm	15 m
Band 9-Cirrus	1.36 - 1.38 µm	30 m
Thermal Infrared Sensor (TIRS)-Built by NASA Goddard Space Flight Centre. Two spectral bands		
Band 10-Thermal Infrared (TIRS) 1	10.6 - 11.19 µm	30 m
Band 11-Thermal Infrared (TIRS) 2	11.5 - 12.51 µm	30 m

Table 2. Metadata of the Landsat 8 satellite image

Variable	Description	Value
K1	Thermal constants, Band 10	774.8853
K2		1321.0789
Lmax	Maximum and Minimum values of	22.00180
Lmin	Radiance, Band 10	0.10033
Qcal max	Maximum and Minimum values of	65535
Qcal min	Quantize Calibration, Band 10	1
Oj	Correction value, Band 10	0.29

where

ϵ = Land Surface Emissivity

P_v = Proportion of Vegetation

0.986 corresponds to a correction value of the equation.

3.6 Step6. Land Surface Temperature (LST) Calculation

Land Surface Temperature (LST) is the radiative temperature which was calculated using Top of Atmosphere brightness temperature, wavelength

of emitted radiance and Land Surface Emissivity. LST was calculated using following equation:

$$LST = (BT / 1) + W * (BT / 14380) * Ln (E)$$

Where

LST=Land Surface Temperature (°C)

BT = Top of atmosphere brightness temperature (°C)

W = Wavelength of emitted radiance

E = Land Surface Emissivity

It should be noted that LST is not equal to the air temperature.

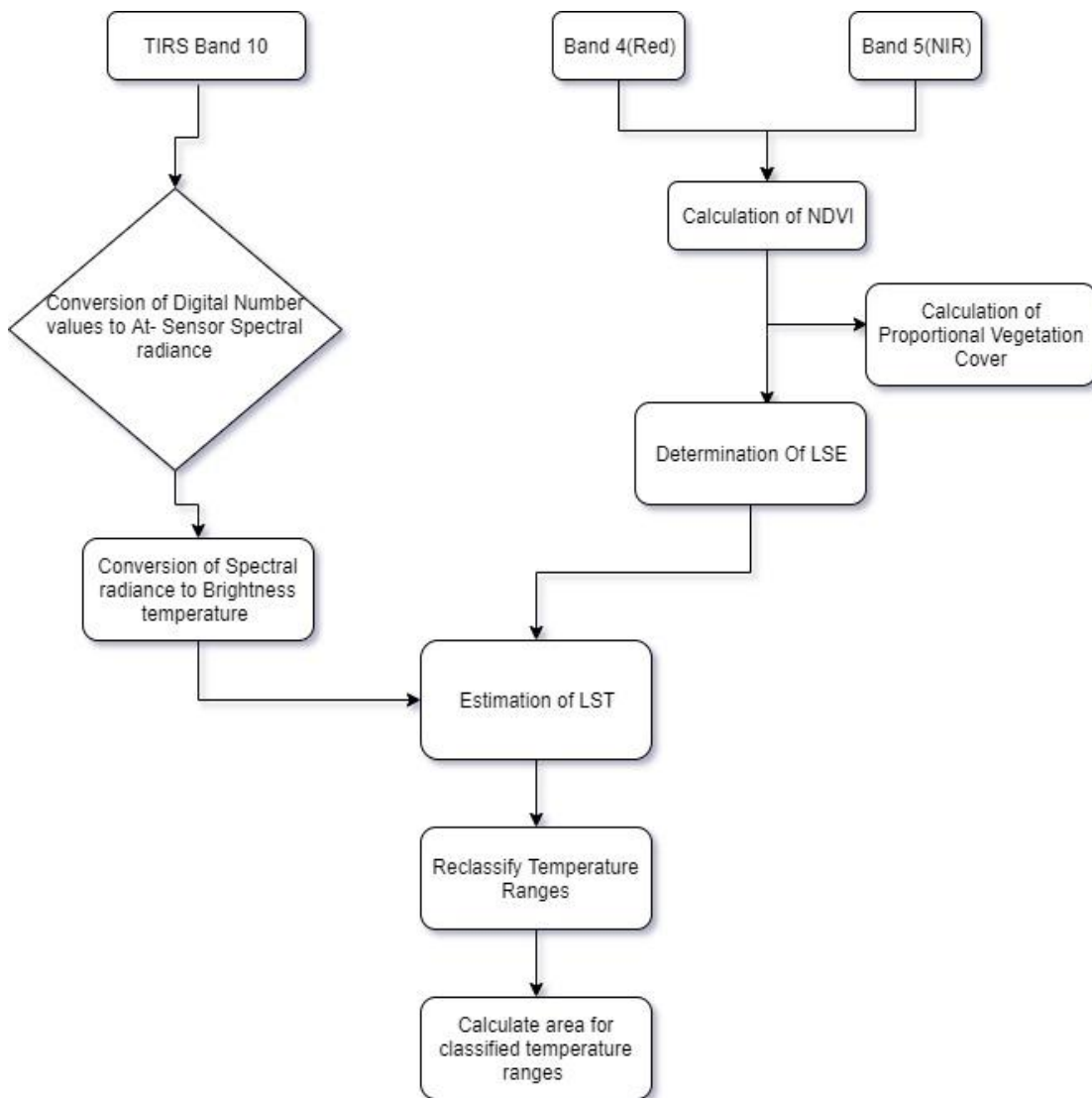


Fig. 2. Flowchart for LST calculation

4. RESULTS AND DISCUSSION

4.1 Brightness Temperature

Brightness Temperature map of 5th May 2019 shows that the temperature ranges from 25.46°C to 56.73 °C (Fig. 3). while brightness temperature map of 28th October 2019 shows that the temperature ranges 18.32 to 33.47°C (Fig. 4).

4.2 Normalized Difference Vegetation Index (NDVI)

NDVI map for 5th May 2019 shows that the NDVI value ranges between -0.24 to 0.56 (Fig. 5). while NDVI map for 28th October 2019 shows that NDVI ranges between -0.13 to 0.53 (Fig. 6).

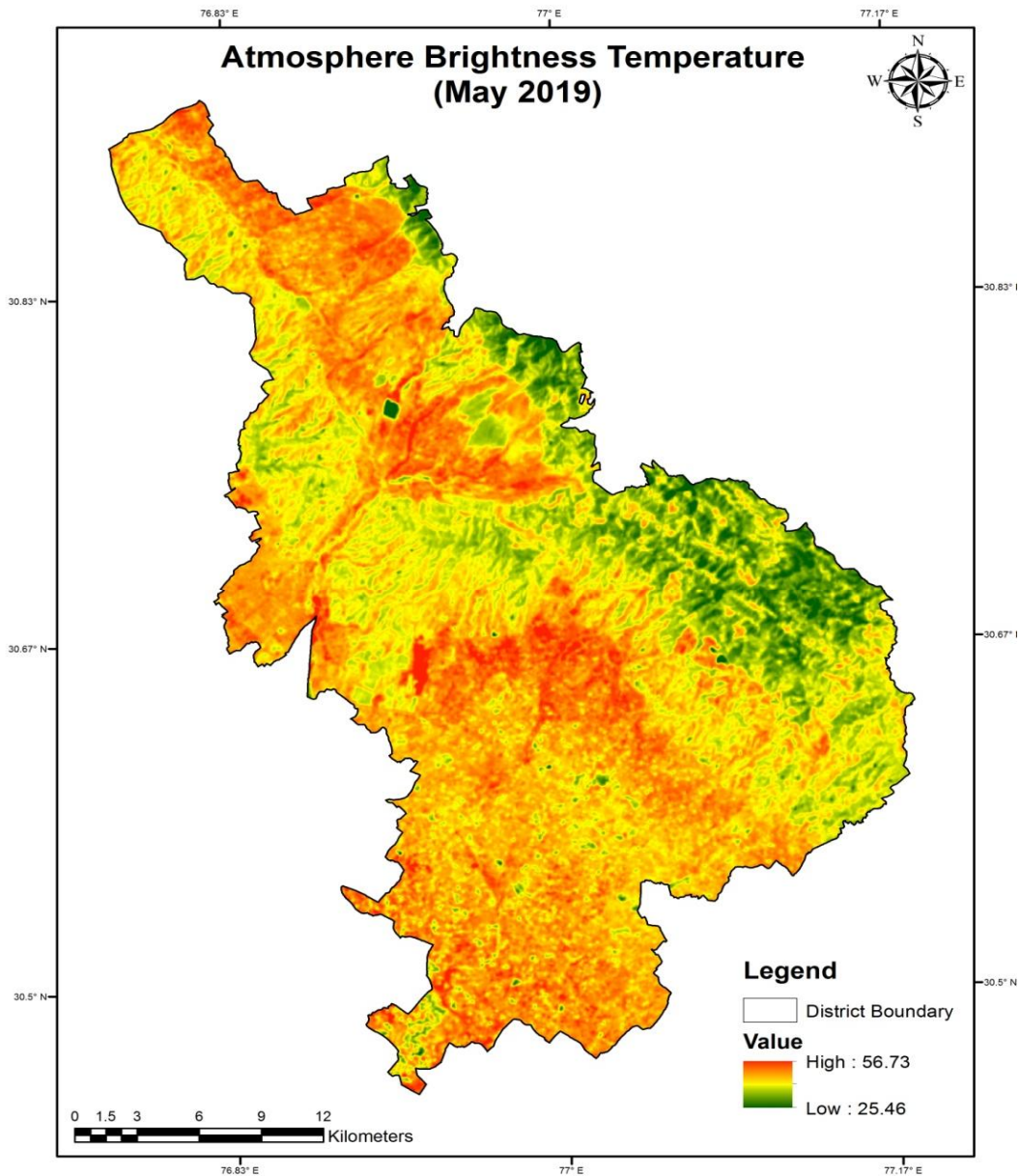


Fig. 3. Brightness temperature map (5th May,2019)

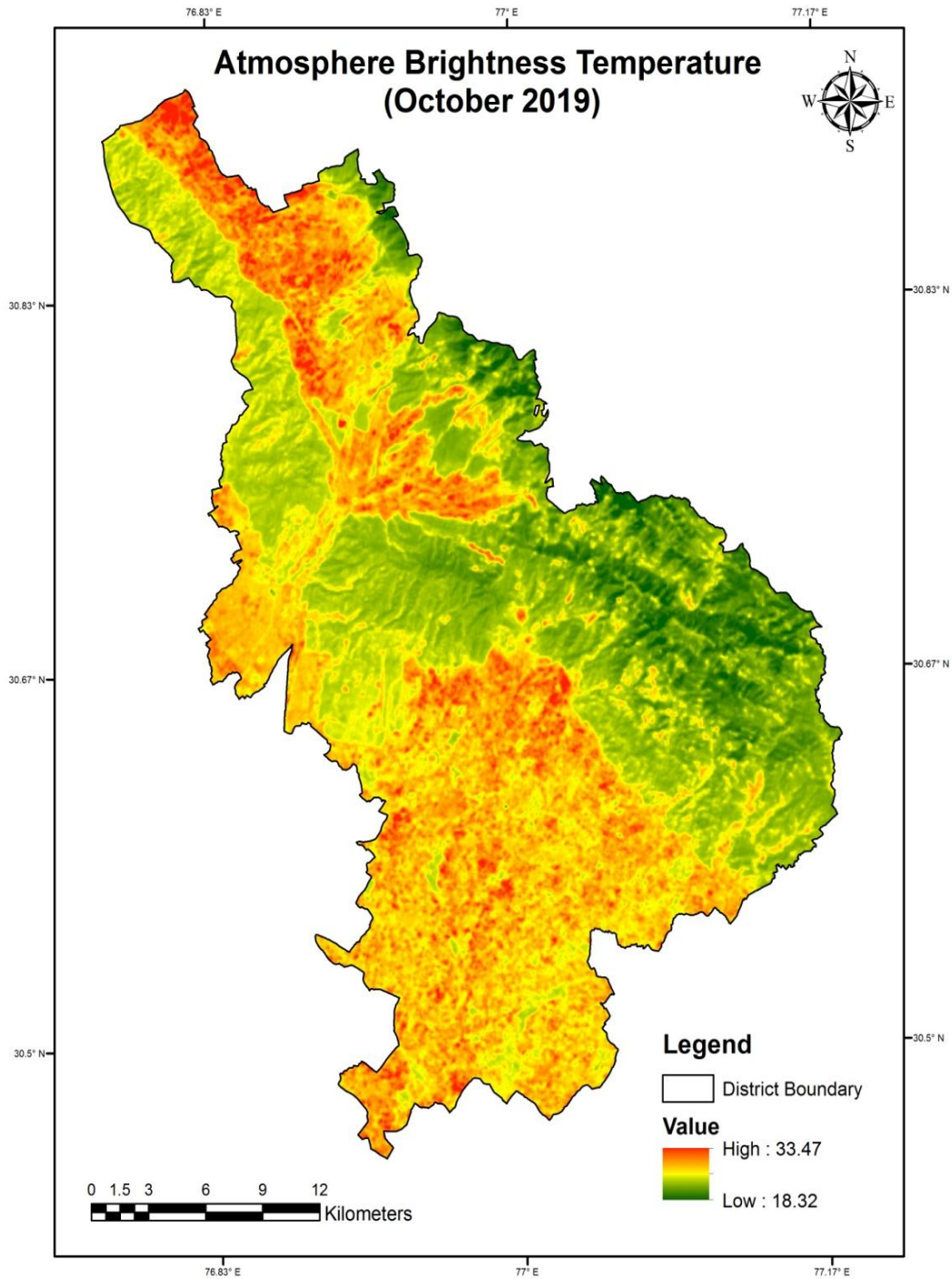


Fig. 4. Brightness temperature map (28th October, 2019)

4.3 Land Surface Emissivity (LSE)

LSE was calculated for 5th May 2019 and 28th October 2019 (Fig. 7 and Fig. 8). LSE in the

study area for 5th May 2019 ranges from 0.98 to 0.99 and for 28th October 2019 LSE ranges 0.98 to 0.99.

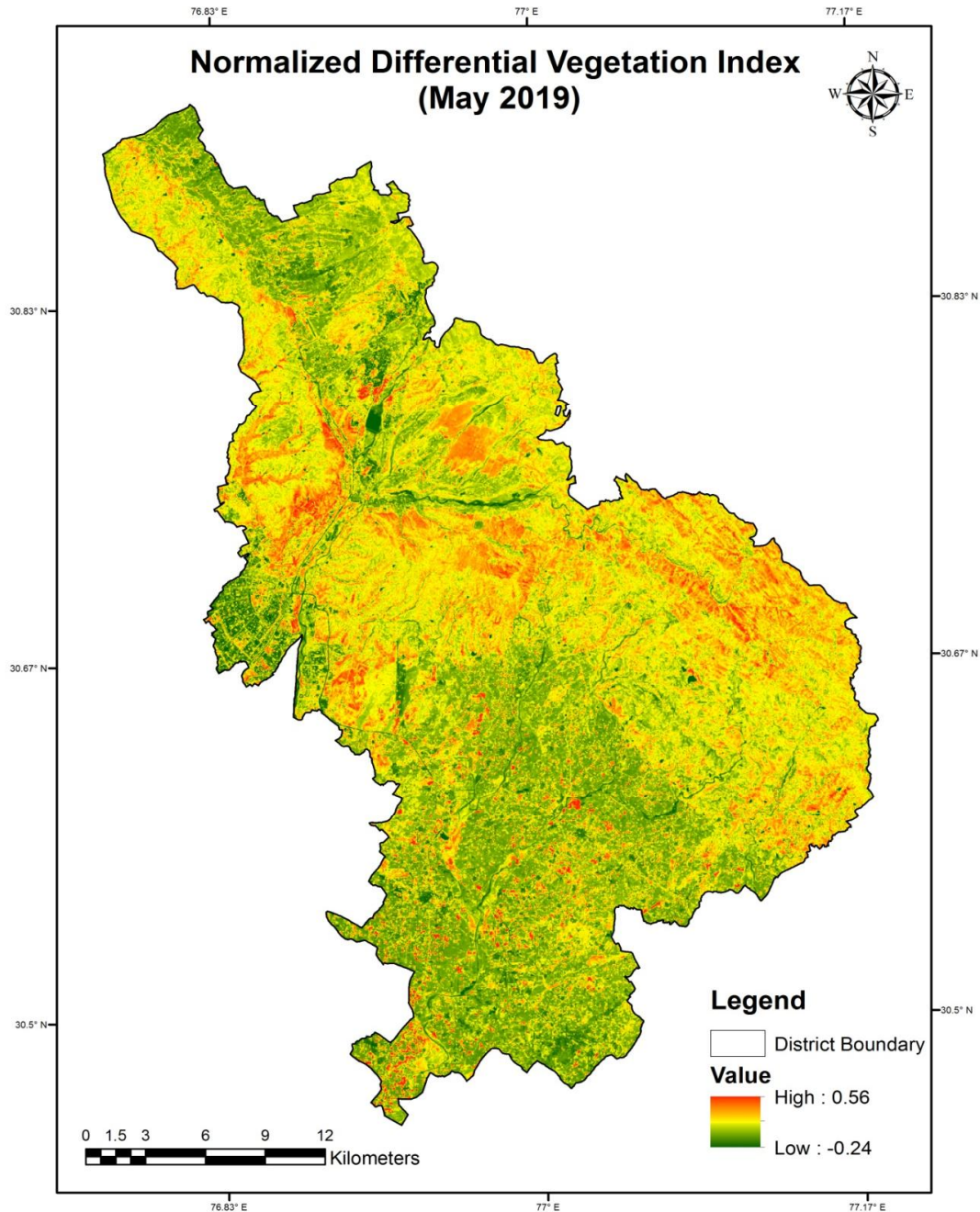


Fig. 5. NDVI map (5th May, 2019)

4.4 Land Surface Temperature

Land Surface Temperature (LST) has been derived using Brightness Temperature and LSE. In the study area on 5th May, 2019 maximum area (279.21 sq km) was falling under LST range 39-41°C and minimum area (67.61 sq

km) was falling under LST range 25.47-34°C (Fig. 9. and Table 3). In the study area on 28th October, 2019 maximum area (433.52 sq km) was falling under LST range 24-26°C and minimum area (1.77 sq km) was falling under LST range 27-33.48°C (Fig. 10. and Table 4).

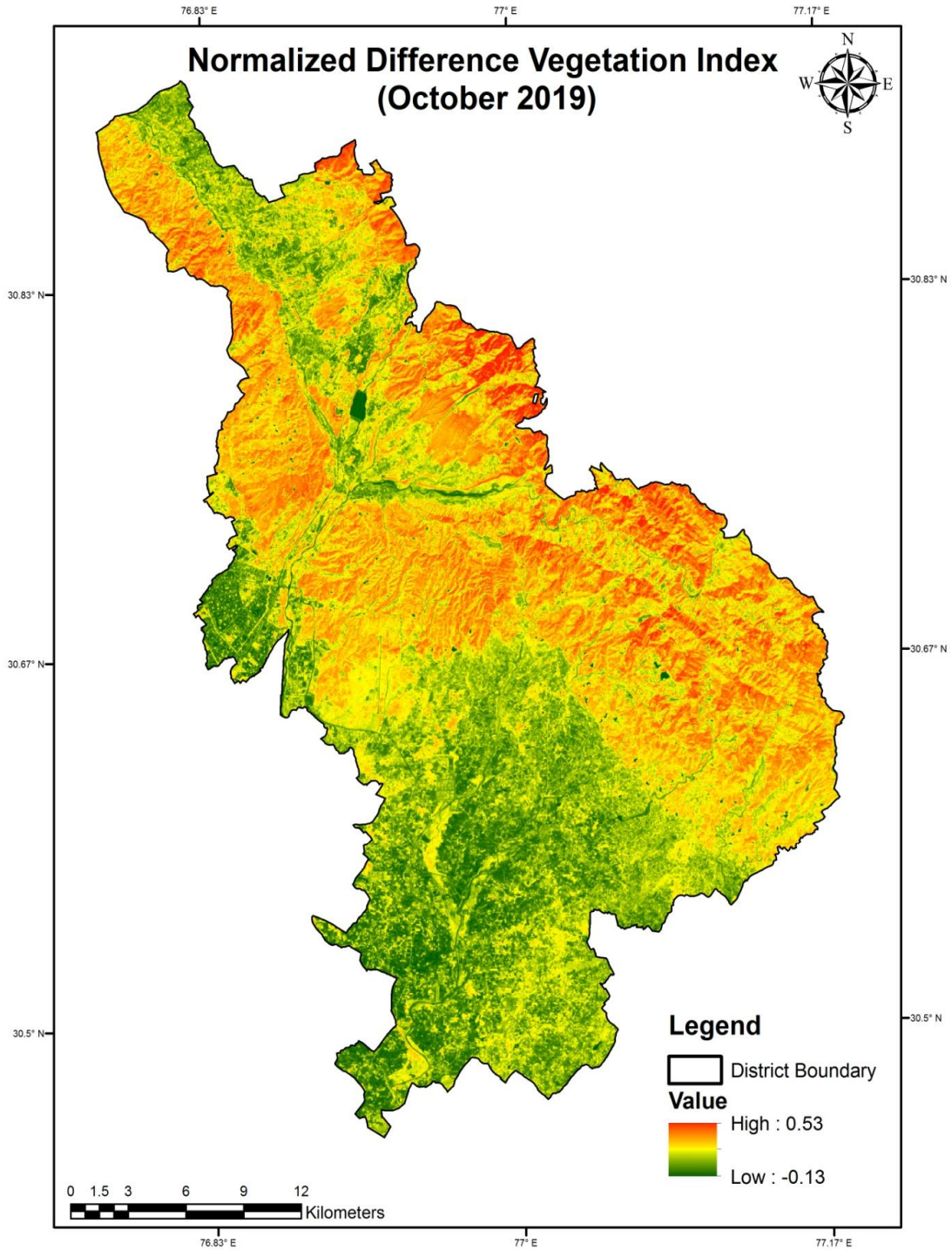


Fig. 6. NDVI map (28 October, 2019)

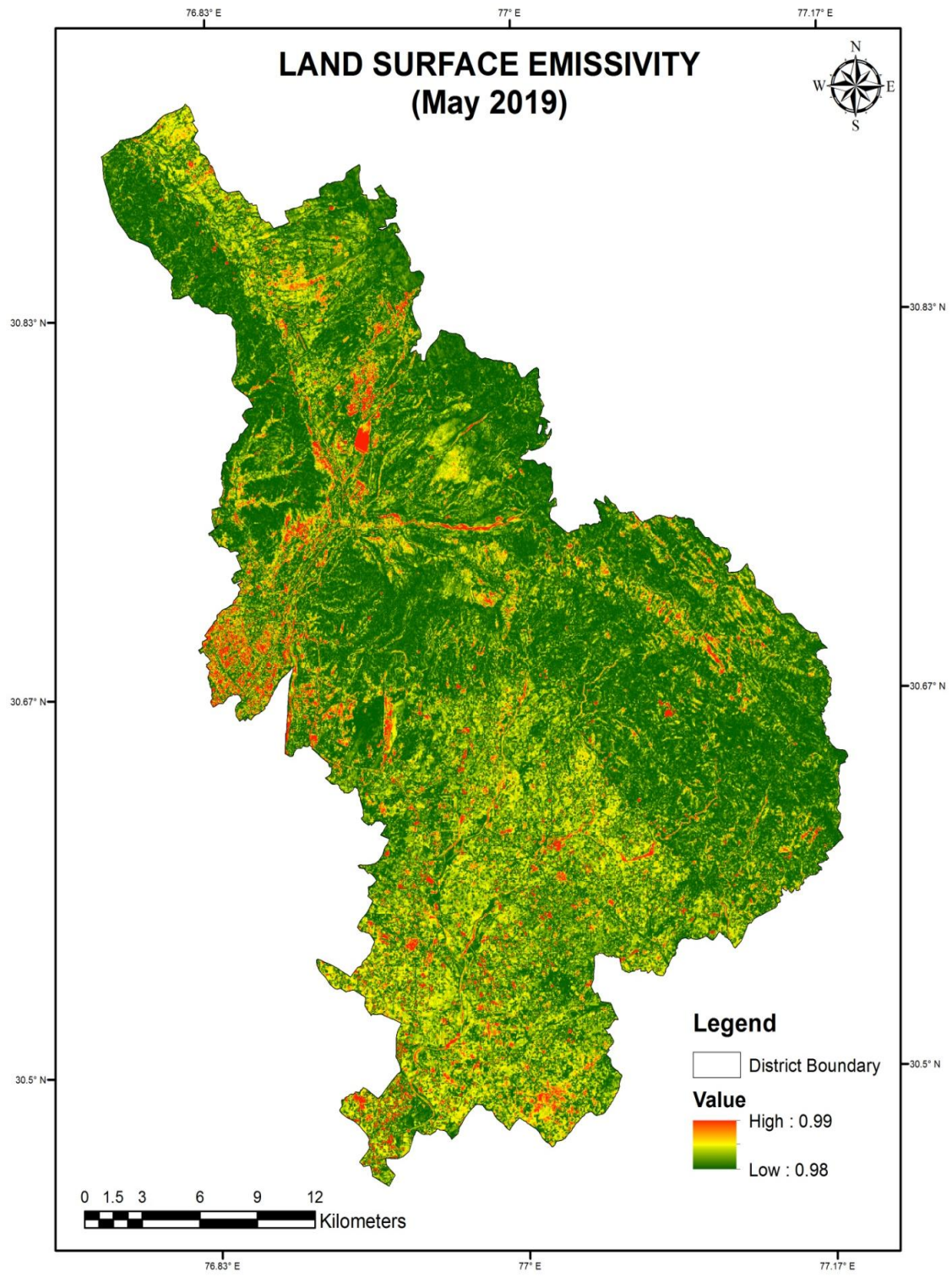


Fig. 7. Land surface emissivity map (5th May, 2019)

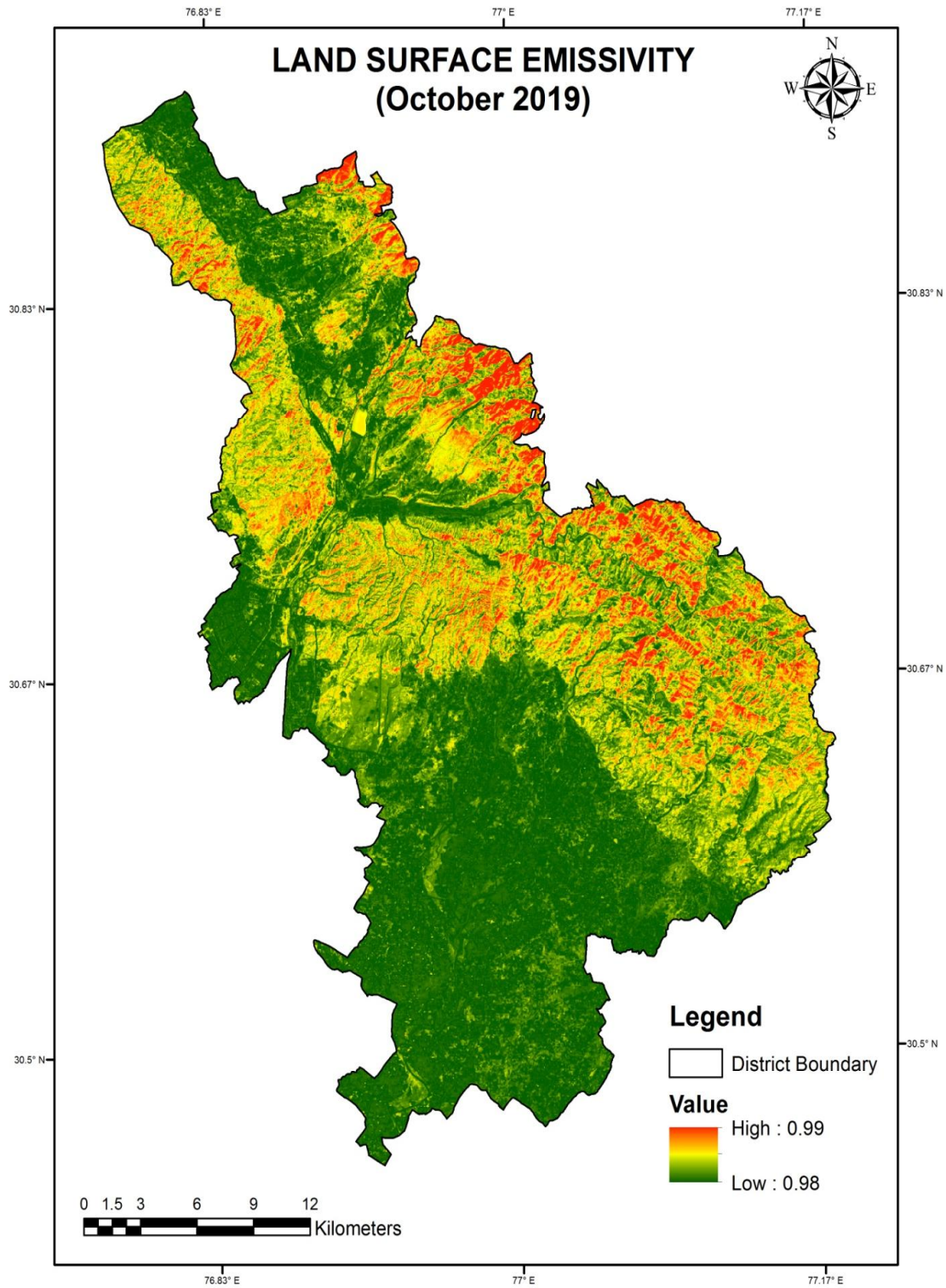


Fig. 8. Land surface emissivity map (28 October, 2019)

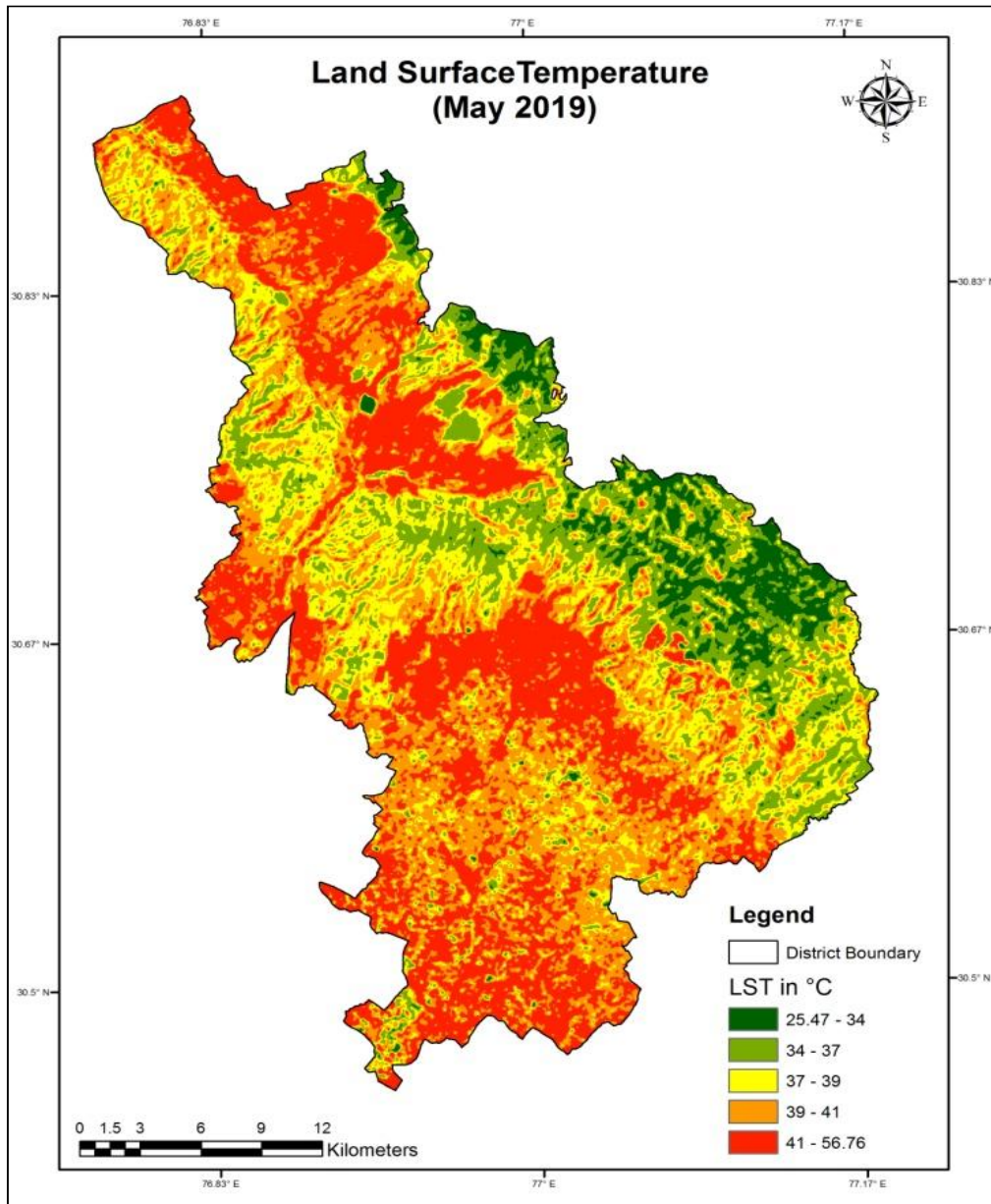


Fig. 9. Land surface temperature (5th May, 2019)

Table 3. Area covered under different LST ranges (5th May, 2019)

Sr. No.	LST (°C) Range	Area (Sq.km)	Percentage (%) of Total Area
1	25.47-34	67.61	7.53
2	34-37	157.19	17.51
3	37-39	232.88	25.93
4	39-41	279.21	31.09
5	41-56.76	161.11	17.94
	Total	898.00	100.00

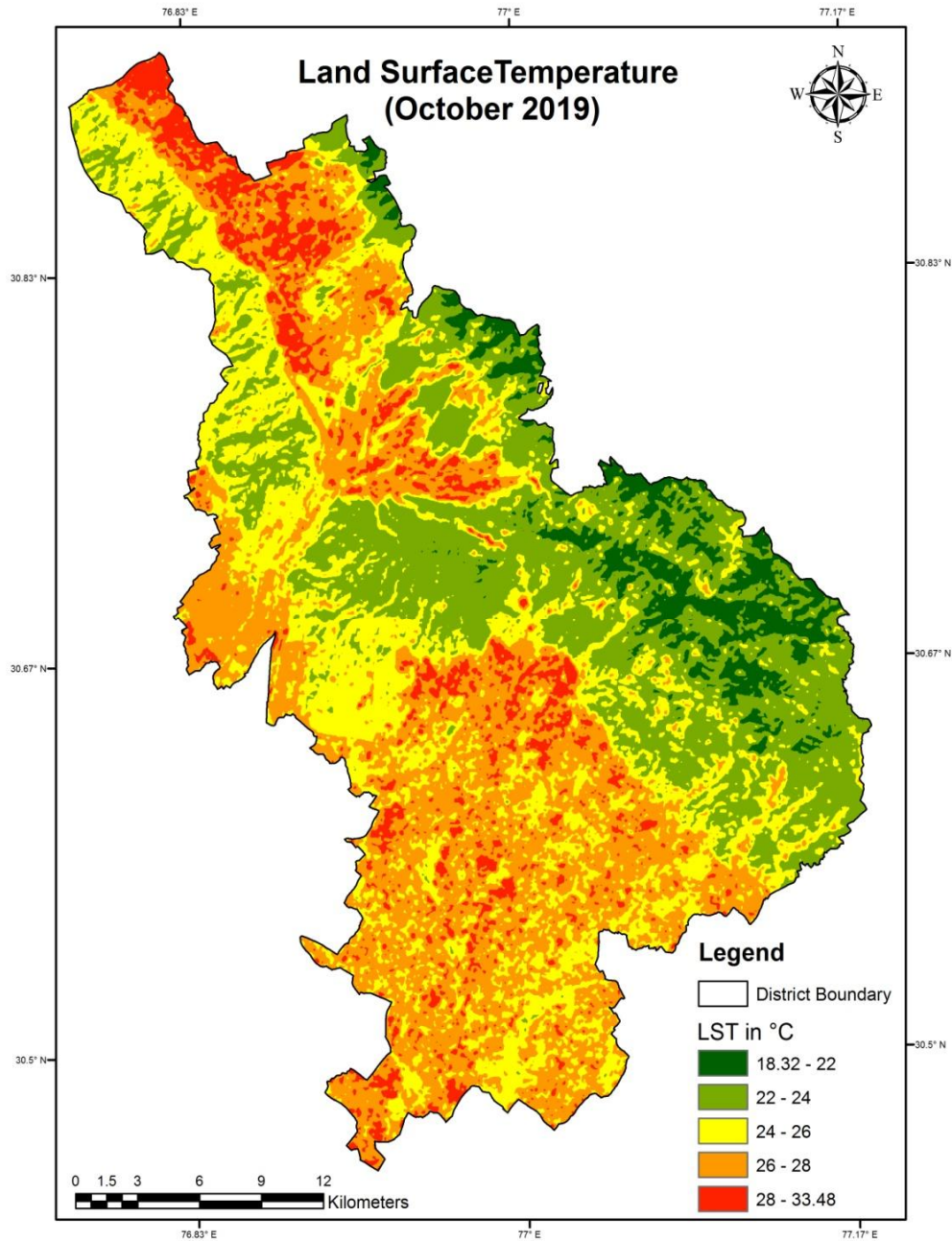


Fig. 10. Land surface temperature (28th October, 2019)

Table 4. Area covered under different LST ranges (28th October, 2019)

Sr. No.	LST (°C) Range	Area (Sq.km)	Percentage (%) of Total Area
1	18.32 - 22	22.33	2.49
2	22-24	319.55	35.58
3	24-26	433.52	48.28
4	26-27	120.83	13.45
5	27-33.48	1.77	0.20
	Total	898.00	100.00

High land surface temperature areas have been observed mainly in cultivated land, scrub land, river course, and built-up land. While low LST areas are found in forest land and water body in the study area. (Fig. 11). On 5th May, 2019 LST more than 40°C at few selected locations is shown in Fig. 12.

4.5 Relationship between Elevation, LULC and LST

In the study one sample of each major land use/land cover class in each elevation range has been selected for LST for 5th May 2019 and 28th October 2019 (Table 5) for relationship analysis. The study shows inverse relationship between

elevation and LST i.e. as elevation is increasing, LST is decreasing in the study area on both dates satellite data i.e. 5th May, 2019 and 28th October, 2019. The study also shows that due to seasonal changes LST has been observed decreasing. For all the land use/ land cover classes on 28th October 2019 as compared to 5th May 2019 LST data (Fig. 13). Relationship between elevation and LST is also shown in Fig. 14. Where digital elevation model (DEM) generated from SRTM 30 m resolution draped on Google Earth satellite data to depict the 3D view of the terrain in which LST is decreasing as elevation increasing. This may be due to inversion of temperature with height in atmosphere.

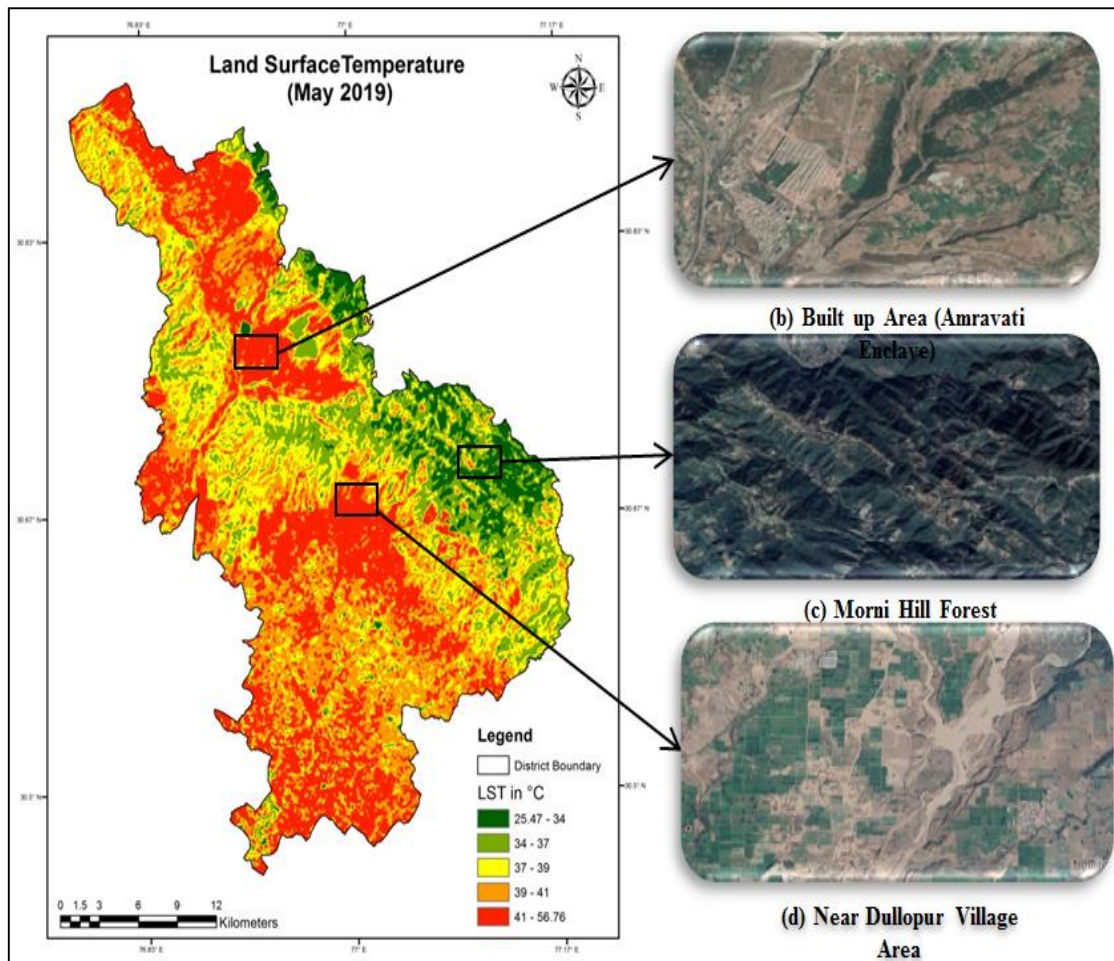


Fig. 11. (a) Land surface temperature in the study area, (b) Google Earth Satellite image of built up area (Amravati Enclave) as shown in box in figure (a), (c) Morni Hill Forest Area as shown in box in figure (a), (d) Dullapur village area as shown in box in figure (a)

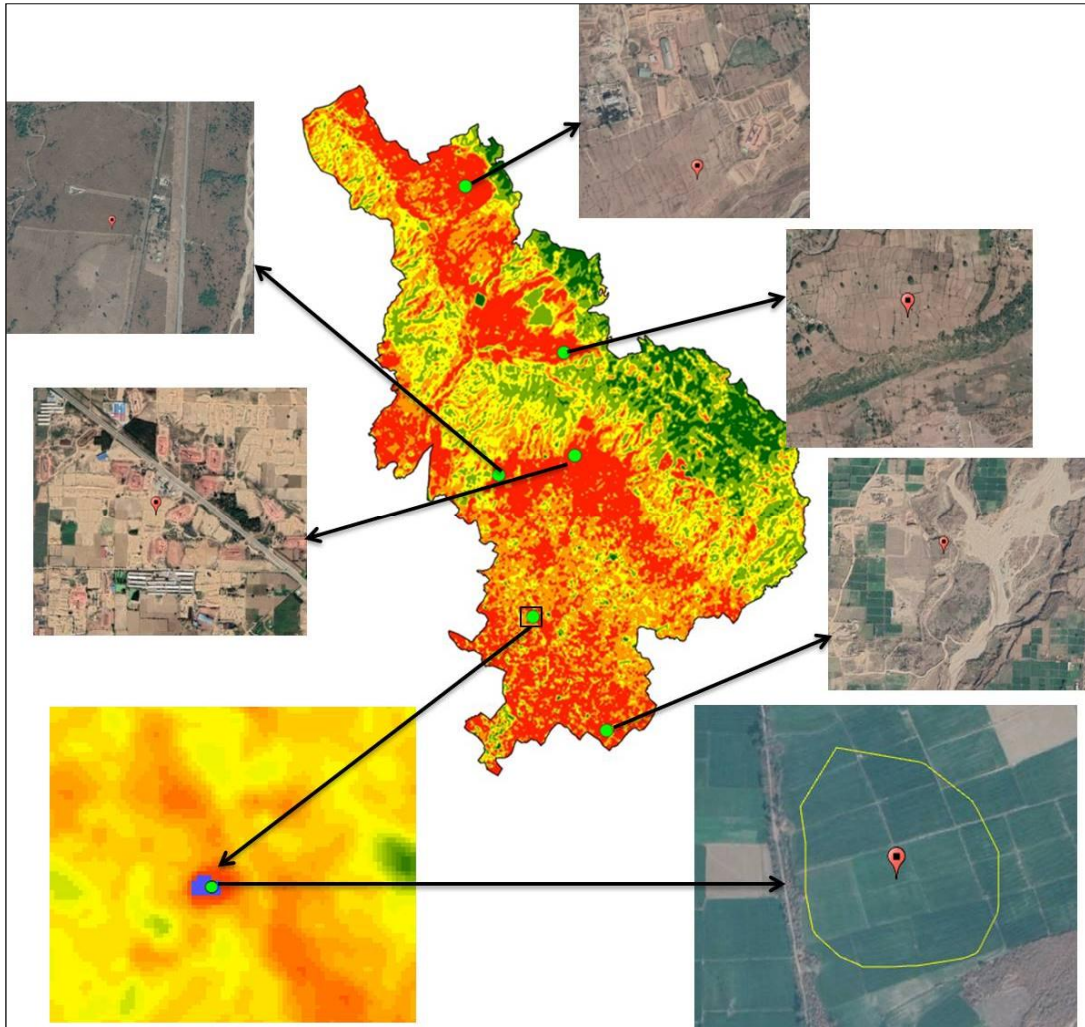


Fig. 12. LST more than 40°C in the study area at few selected locations. High LST areas are marked in red on the Google Earth satellite image and highest LST (56.70 °C) area in yellow polygon in the study area which may be due to some burning activity on 5th May, 2019 at that location

4.6 Study Limitations and Difficulties

This study examined the relationships between LST, different land use types and Elevation Ranges. After retrieving the LST, the results needed to be verified to ensure the correctness of the results. There are Two common methods for verifying the result: The first is a to compare the retrieved LST with the MODIS LST product, called the cross-comparison method. The advantage of this method is that MODIS surface temperature products are free and easy to obtain. The disadvantage is that MODIS surface temperature products data may loss in some areas, and because the spatial resolution

is not high, the correctness of the retrieved results can only be roughly verified. The second method is to compare with ground observation data. The advantage of this method is that it is simple and accurate. The disadvantage is that it is tough and expensive to obtain verification data, and it is not feasible for studying past surface temperatures, because it is impossible to return to the time of satellite overpass to measure accurate surface temperature. Since the data of MODIS LST products in this study area are missing, and the air temperature data for the local meteorological station were not available at the specific time of the study area.

Table 5. Relationship between elevation, LULC and LST

Elevation (m)	May 2019 and October 2019 Land Surface Temperature (LST) (Degree Celsius) of one sample of each major Landuse/ Land cover class in each elevation range in Panchkula District											
	Bulitup Land		Water Body		Forest Land		Cultivated Land		Scrub Land		River Course	
	May	Oct.	May	Oct	May	Oct	May	Oct	May	Oct	May	Oct
288-400	43.86	28.21	38.52	26.3	39.12	24.01	54.05	28.06	44.42	28.48	44.5	27.71
400-550	41.7	27.43	36.96	24.23	38.45	23.91	44.09	27.7	41.46	26.39	43.34	27.43
550-700	41.53	26.7	37.61	23.38	37.28	22.85	43.03	27.03	40.6	25.82	41.5	27.11
700-850	39.1	25.98	36.61	24.41	35.62	22.57	41.73	26.13	40.93	25.86	41.91	26.05
850-1000	36.1	23.33	33.06	22.54	30.89	21.22	36.71	24.08	37.48	23.28	39.11	23.85
1000-1500	35.86	22.13	33.18	21.64	27.28	19.07	38.12	21.65	33.41	21.7	30.41	20.67

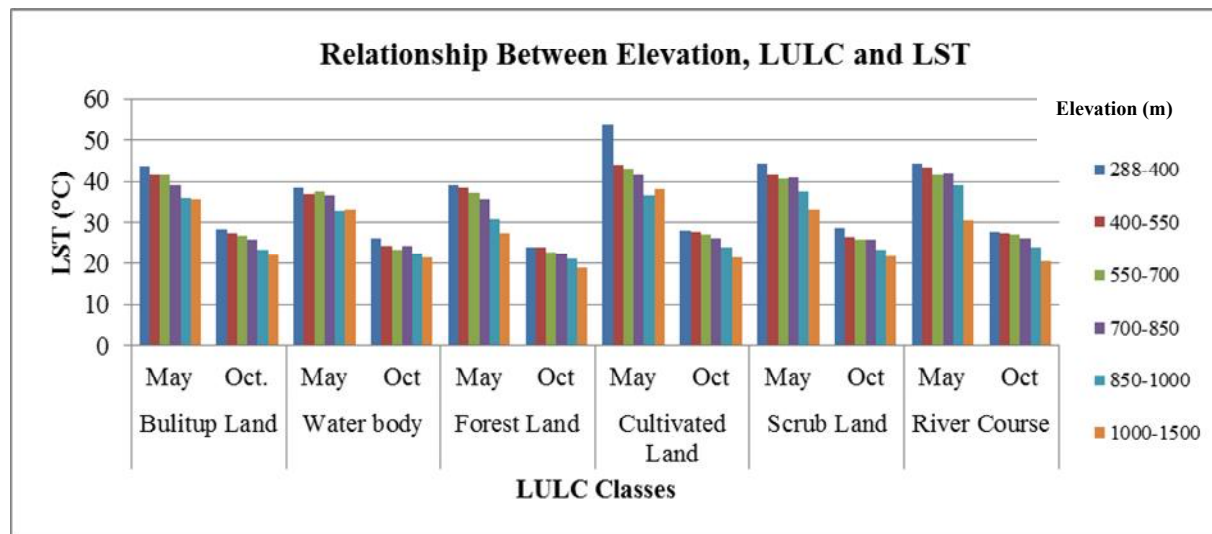


Fig. 13. Relationship between elevation, LULC and LST in the study area

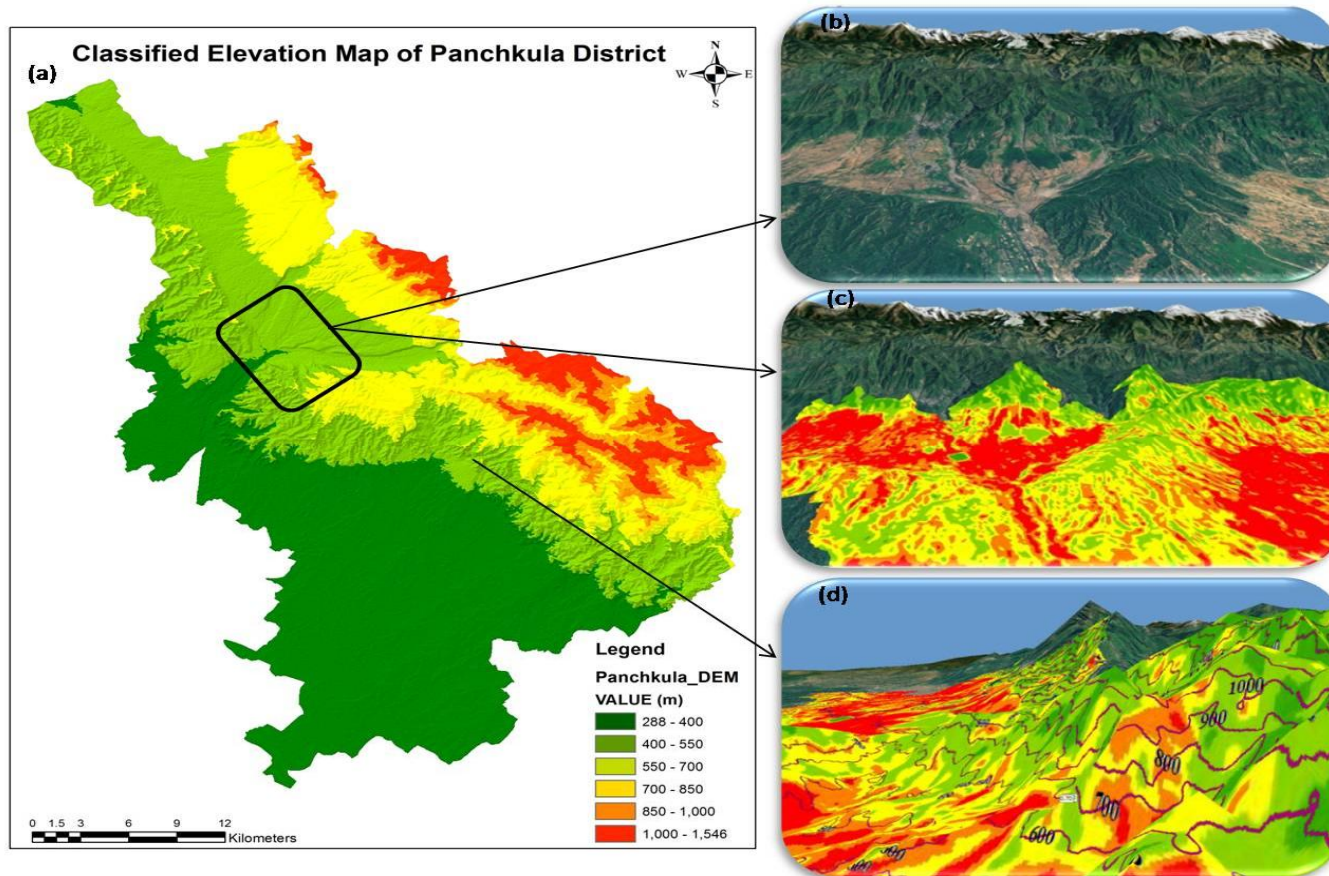


Fig. 14. Relationship between Elevation and LST. Fig. 14 (a). represents classified elevation ranges generated from SRTM 30 m DEM while Fig. 14 (b) is a satellite view of the box area on Fig 14 (a). in Fig. 14 (c). LST is draped on satellite image for 3D view and in Fig. 14 (d). contour at 100m interval draped on LST and satellite image for 3D view

5. CONCLUSIONS

Highest LST has been observed in cultivated land on 5th May 2019 and scrub land on 28th Oct 2019. Lowest LST has been observed of water body on 5th May 2019 and forest land on 28th October 2019. LST of all the land use/land cover classes on 28th Oct 2019 is lower than LST 5th May 2019 land use/land cover classes due to seasonal variation. The study also shows that as the elevation increases, LST is decreasing in the study area. The study can be used to monitor the land surface temperature variation of various land use/land cover classes in the study area. The methodology can be replicated for large urban areas for delineating heat islands like hot work industries; thermal springs, seismic movement, volcanic activity, coal mine fire, stubble burning and forest fires.

ACKNOWLEDGEMENTS

The authors would like to express their sincere thanks to the reviewers for their constructive suggestions, comments and helps. Authors also thankfully acknowledge the USGS and Google Earth for using their satellite data in the research work.

COMPETING INTERESTS

Authors have declared that no competing interests exist.

REFERENCES

1. Deng Yuanhong, Wang Shijie, Bai Xiaoyong, Tian Yichao, Wu Luhua, Xiao Jianyong, et al. Relationship among land surface temperature and LUCC, NDVI in typical karst area, Scientific Reports. 2018;8(641):1-12.
DOI: <https://doi.org/10.1038/s41598-017-19088-x>
2. Anandababu D, Purushothaman BM, Babu S Suresh. Estimation of land surface temperature using LANDSAT 8 data. International Journal of Advance Research, Ideas and Innovations in Technology. 2018;4(2):177-186.
Available:<https://www.ijariit.com/manuscripts/v4i2/V4i2-1195.pdf>
3. Prasad Rajendran, Mani K. Estimation of spatial variability of land surface temperature using Landsat 8 imagery. The International Journal of Engineering and Science (IJES), 2015;4(11):19-23.
Available:<http://www.theijes.com/papers/v4-i11/Version-3/D041103019023.pdf>
4. Jeevalakshmi D, Reddy S, Narayana Manikiam B. Land surface temperature retrieval from LANDSAT data using emissivity estimation. Int.J. Applied Engineering Research. 2017;12(20):9679-9687.
Available:https://www.researchgate.net/publication/329683798_land_surface_temperature_retrieval_from_LANDSAT_data_using_emissivity_estimation
5. Rajeshwari A, Mani ND. Estimation of land surface temperature of Dindigul District using Landsat 8 data. Int. J. Research in Engineering and Technology. 2014;03(05):122-126.
Available:<https://ijret.org/volumes/2014v03/i05/IJRET20140305025.pdf>
6. Avdan Ugur, Jovanovska Gordana. Algorithm for automated mapping of land surface temperature using LANDSAT 8 satellite data. Journal of Sensors, 2016;1480307:1-8,
DOI:
<https://doi.org/10.1155/2016/1480307>.
(<https://giscrack.com/how-to-calculate-land-surface-temperature-with-landsat-8-images/>)
7. Candy B, Saunders RW, Ghentm D, Bulgin CE, The impact of satellite-derived land surface temperatures on numerical weather prediction analyses and forecasts. Journal of Geophysical Research: Atmospheres. 2017;22(18):9783-9802.
DOI:
<https://doi.org/10.1002/2016JD026417>
8. Hope AS, McDowell TP. The relationship between surface temperature and a spectral vegetation index of a tall grass prairie: effects of burning and other landscape controls. Int. J. Remote Sens. 1992;13:2849-2863.
DOI:
<https://doi.org/10.1080/01431169208904086>
9. Jose A, Sobrino Juan C, Jimenez Munoz, Guillem Sòria, Mireia Romaguera, Luis Guanter, et al. Land surface emissivity retrieval from different VNIR and TIR

- Sensors. IEEE Transactions on Geosciences and Remote Sens. 2008; 46(2):316-327.
DOI: 10.1109/TGRS.2007.904834
10. Julien Y, Sobrino JA, Verhoef W. Changes in land surface temperatures and NDVI values over Europe between 1982 and 1999. Remote Sensing of Environment. 2006;103:43-55.
DOI:
<https://doi.org/10.1016/j.rse.2006.03.011>
 11. Juan C, Jiménez Muñoz, Jose Sobrino A, Skokovic Drazen, Mattar Cristian, Cristobal Jordi. Land surface temperature retrieval methods from Landsat-8 thermal infrared sensor data. IEEE Geoscience and Remote Sensing Letters. 2014;11(10): 1840-1843.
DOI: 10.1109/LGRS.2014.2312032
 12. Juan Carlos, Jimenez Muñoz, Sobrino Jose A. Split-window coefficients for land surface temperature retrieval from low-resolution thermal infrared sensors. IEEE Geoscience and Remote Sensing Letters. 2008;5(4):806-809.
DOI: 10.1109/LGRS.2008.2001636
 13. Chitade Anil, Katyar SK. Impact analysis of open cast coal mines on land use/ land cover using remote sensing and GIS technique: A case study. Int. J. Engineering Science and Technology. 2010;2(12):7171-7176.
Available:https://www.researchgate.net/publication/50384275_IMPACT_ANALYSIS_OF_OPEN_CAST_COAL_MINES_ON_LAND_USE_LAND_COVER_USING_REMOTE_SENSING_AND_GIS_TECHNIQUE_A_CASE_STUDY
 14. Latif Md Shahid. LST retrieval of Landsat-8 data using split window algorithm-a case study of Ranchi District. Int.J.Engineering Development and Research, 2014;2(4): 3840-3849.
Available:<https://www.ijedr.org/papers/IJEDR1404073.pdf>
 15. Prakasam C. Land use and land cover change detection through remote sensing approach: a case study of Kodaikanal taluk, Tamil Nadu. Int.J.Geomatics and Geosciences, 2010;1(2):150-158.
Available:<http://www.ipublishing.co.in/jggsvo11no12010/EIJGGS1015.pdf>
 16. Ren Zhibin, Zheng Haifeng, He Xingyuan, Zhang Dan, Yu Xingyang, Estimation of the relationship between urban vegetation configuration and land surface temperature with remote sensing. J. Ind. Soc. Remote Sens. 2015;43(1):89-100.
DOI:10.1007/s12524-014-0373-9.
 17. Sobrino JA, Raissouni N. Toward remote sensing methods for land cover dynamic monitoring: application to Morocco. Int.J. Remote Sens., 2010;21(2):353-366.
DOI:
<https://doi.org/10.1080/014311600210876>
 18. Trigo Isabel F, Boussetta Souhail, Viterbo Pedro, Balsamo Gianpaolo, Beljaars Anton, Sandu Irina. Comparison of model land skin temperature with remotely sensed estimates and assessment of surface- atmosphere coupling. Journal of Geophysical Research: Atmospheres. 2015;120(23):96-111.
DOI:
<https://doi.org/10.1002/2015JD023812>
 19. Wang Aihui, Barlage Michael, Zeng Xubin, Draper Clara Sophie. Comparison of land skin temperature from a land model, remote sensing, and in situ measurement. Journal of Geophysical Research: Atmospheres, 2014;119(6):3093-3106.
DOI:10.1002/2013JD021026.
 20. Mallick Javed, Kant Yogesh, Bharath BD. Estimation of land surface temperature over Delhi using Landsat-7 ETM+. J. Ind. Geophys. Union, 2008;12(3):131-140.
Available:<http://citeseerx.ist.psu.edu/viewdoc/download?doi=10.1.1.585.9524&rep=rep1&type=pdf>
 21. Meijun Jin, Junming Li, Caili Wang, Ruilan Shang, A practical split-window algorithm for retrieving land surface temperature from Landsat-8 data and a case study of an urban area in China. Remote Sens., 2015;7(4):4371-4390;
DOI: 10.3390/rs70404371
 22. Randrianjatovo RN, Rakotondraompiana S, Rakotoniaina S. Estimation of land surface temperature over reunion island using the thermal infrared channels of Landsat-8. IEEE Canada International Humanitarian Technology Conference - (IHTC).2014;1-4.
DOI: 10.1109/IHTC.2014.7147516

23. Sun Qinqin, Wu Zhifeng, Tan Jianjun, The relationship between land surface temperature and land use/land cover in Guangzhou, China, Environ Earth Sci. 2012;65:1687–1694.
DOI: 10.1007/s12665-011-1145-2.

© 2020 Kumar and Kumar; This is an Open Access article distributed under the terms of the Creative Commons Attribution License (<http://creativecommons.org/licenses/by/4.0>), which permits unrestricted use, distribution, and reproduction in any medium, provided the original work is properly cited.

Peer-review history:
The peer review history for this paper can be accessed here:
<http://www.sdiarticle4.com/review-history/66425>